Sequential Interconnected Interpenetrating Polymer Networks of Polyurethane and Polystyrene. 1. Synthesis and Chemical Structure Elucidation†

S. B. Pandit and V. M. Nadkarni*

Polymer Science and Engineering Group, Chemical Engineering Division, National Chemical Laboratory, Pune 411 008, India

Received July 28, 1993; Revised Manuscript Received November 22, 1993®

ABSTRACT: In-situ sequential semi-interconnected interpenetrating polymer networks (IPNs) based on well-defined unsaturated poly(ester–urethane) (PU) and polystyrene (PS) were synthesized at PU/PS ratios of 100/0, 90/10, 80/20, 70/30, and 50/50, in order to study the effect of length of PS intranetwork bridges on the structure. The structure of these IPNs was studied using various characterization techniques such as swelling behavior in binary solvent mixtures, wide angle X-ray diffraction (WAXD), and solid state ^{13}C nuclear magnetic resonance (NMR) spectroscopy. The swelling studies showed that PS intranetwork bridges influence the size of the network cages formed. The swelling studies in a binary solvent mixture indicated that the PS intranetwork bridges of up to 6 styrene units (SU) in length are present in the stretched configuration. WAXD studies showed that the effective distance between the chains (d_{eff}) increased up to the intranetwork bridge length of 6 SU and decreased on a further increase in the bridge length. Thus, both swelling and WAXD studies indicated that in the IPNs containing longer PS intranetwork bridges the PS chains are in a coiled configuration. This fact was confirmed by ^{13}C NMR spectroscopy which showed the increased mobility of the PS bridges in the case of the IPNs containing a higher PS content. On the basis of these results, it is proposed that the PU cages are amorphous and present in a coiled configuration, the IPNs containing up to 30% PS had cages containing stretched PS bridges and the IPN containing 50% PS had cages containing coiled PS bridges.

Introduction

Interpenetrating polymer networks[1] (IPNs) are a class of materials formed by combination of two polymers, at least one of which is a thermoset. Thus a typical IPN consists of a multicomponent network of two or more polymers which are entangled to form physical cross-links but there is no covalent bonding between the two networks. The IPNs formed by sequential polymerization of the two polymers are termed sequential IPNs (SIPNs). The sequential IPN formed by trapping the monomer of the second network forming polymer during the formation of the first polymer network is termed an in-situ sequential IPN. If, during in-situ sequential IPN formation of polyurethane (PU) and polystyrene (PS), the PU network contains sites of unsaturation which can react with styrene, then the PU network chains are connected with each other by polystyrene. Such IPNs in which the two network chains are bonded to each other through chains of another polymer are termed interconnected IPNs (IcIPNs). The bridges of polystyrene formed by reaction of styrene with the sites of unsaturation present on the adjacent chains of the PU network are termed as intranetwork bridges.

The intranetwork bridges formed in the interconnected IPNs can affect the IPN structure and properties greatly. Sperling and co-workers[2] have shown that relatively low levels of grafting can cause significant changes in morphology and behavior of the final product. A similar observation was made by Frisch et al.[3] in the case of epoxy/acrylic IPNs with intentional grafts.

Sperling et al.[4] have studied IPNs formed from castor oil based polyurethane (COPU) and PS. It was observed that the tensile strength and modulus of the IPNs increased with the increasing amount of PS. However, other studies carried out using similar compositions[5] showed that the tensile strength and modulus of the IPNs decreased and the molecular weight between cross-links (M_c) increased, as a result of an increase in the PS content. This descrepancy may result from the intranetwork grafting or cross-linking by PS onto the unsaturation sites of the castor oil moiety. If this is taken into consideration, the properties of COPU/PS IPNs may be rationalized and the sensitivity of the IPN properties to the method of synthesis can be explained. In order to investigate this particular aspect, we have synthesized an unsaturated polyester with a known structure. The synthesized unsaturated polyester has reactive double bonds so that during the formation of the IPNs based on unsaturated polyester–urethane and PS the grafting will take place between PU and PS. With this strategy it is possible to assess the influence of the number and lengths of intranetwork bridges on the structure of the IPN formed. In this communication, the effect of intranetwork grafting on the structure of the interconnected in-situ sequential IPNs based on PU and PS is reported and a cage structure of the IPNs is proposed. In subsequent papers, the variation in the properties of these IPNs with chemical composition will be reported in the context of the proposed structure.

Experimental Section

Synthesis. Materials. The chemicals used in this study are listed in Table 1. All the chemicals were chemically pure grade and were used without further purification. TMP was used after drying in the vacuum desiccator over anhydrous calcium chloride ($CaCl_2$). Styrene was used after drying over sodium sulfate (Na_2SO_4).

Unsaturated Polyester Polyol Synthesis. The reactants PEG 200 (2 equiv) and maleic anhydride (1 equiv) were used for the synthesis. These were weighed into the round bottom flask. PTSA catalyst at a concentration of 0.3% by moles of acid was added to the reaction mixture. Hydroquinone (200–300 ppm) was also added before the start of the reaction to inhibit the free radical reaction of the anhydride, which can take place during the polyester synthesis. The experimental assembly was set up

* To whom all correspondence should be addressed.
† NCL Communication No. 5770.
® Abstract published in *Advance ACS Abstracts*, March 15, 1994.

0024-9297/94/2227-4583$04.50/0

Table 1. List of Raw Materials

sr no.	name of raw materials	abbrev. code	mol wt	supplier
1	poly(ethylene glycol)	PEG	200[a]	M/s NOCIL India Ltd., India
2	maleic anhydride	MAN	98.06	M/s Loba Chamie Ltd., India
3	toluene diisocyanate	TDI	174.16	M/s Bayer AG, Germany
4	tri(hydroxymethyl)propane	TMP	134.18	M/s Wilson Laboratories Ltd., India
5	styrene	styrene	104.15	M/s S. D. Fine Chemicals Ltd., India
6	benzoyl peroxide	BPO	242.23	M/s Loba Chemie Ltd., India

[a] Molecular weight reported is number average molecular weight ($\bar{M}_n$) as reported by the supplier.

Table 2. Characteristics of PUP-2

appearance	pale yellow, viscous liquid
viscosity at 27 °C (cps)	3350
acid value (mg of KOH/g of sample)	1.96
hydroxyl value (mg of KOH/g of sample)	196.88
$\bar{M}_n$ by VPO	880

after weighing in all the reactants. The reactants were then heated from room temperature to 100 °C at the rate of about 3 °C/min with continuous stirring and nitrogen purge from the start. About 30 mL of xylene was added to the reaction mixture (550 g) at the start of the reaction for azeotropic removal of water of condensation. After the temperature of 100 °C was attained, the temperature of the reaction mixture was further raised to 180 °C by adjusting the heating rate to 1 °C/min. The temperature was then kept constant at 180 °C for 2 h. The temperature at which the water of condensation starts coming out was recorded. The reaction temperature was then raised to 200 °C at the rate of 1 °C/min and kept constant for 3 h. The temperature was further raised to 220 °C at a heating rate of 1 °C/min, and the acid value of the product was monitored. When the acid value of the product reached below 5 mg of KOH/g of sample, the heating was discontinued. The reaction mixture was cooled to 180 °C and the reaction was then continued under reduced pressure of about 50 mmHg, to remove xylene and traces of water of condensation till an acid value of less than 2.0 mg of KOH/g was reached. The vacuum was then released, and the product was allowed to cool under stirring and an inert atmosphere. The polyester was allowed to cool to about 60 °C in the reactor and then it was transferred to an amber-colored bottle by filtering through muslin cloth. This unsaturated polyester polyol was coded as PUP-2 and characterized for acid value, hydroxyl value, viscosity, and VPO. The details of characterization procedures and the spectroscopic study performed to determine chemical structure of the polyol are reported in the earlier communication.[6] The characteristics of PUP-2 are summarized in Table 2.

IPN Synthesis. Four hydroxyl equivalents of polyol PUP-2 and one hydroxyl equivalent of TMP were mixed in a degassing chamber. The mixture was heated to 70 °C to dissolve the TMP in PUP-2 and degassed at 80 °C for at least 1h with mechanical stirring at a reduced pressure of 1–2 Torr. The mixture was then cooled to room temperature and 5 isocyanate equiv. of TDI was added. The reaction mixture was mixed thoroughly and degassed further for 5 min. The reaction exotherm during this step was about 40–45 °C.

In a separate beaker, the desired amount of styrene monomer containing 2% BPO was weighed and dried over anhydrous Na_2SO_4. The required quantity of the degassed PU was then added to this mixture with constant stirring to obtain a homogeneous mixture which was then cast into an open aluminum mold of size 250 mm × 250 mm × 2 mm.

The IPNs were cured at room temperature for 24 h to complete the PU network formation, followed by a postcure at 90 ± 2 °C for 20 h and at 120 ± 2 °C for 6 h to complete the polymerization of styrene. The loss of styrene monomer during the complete curing cycle was found to be around 2–4% based on styrene weight. Using this procedure five IPNs were prepared by varying the PU/PS (w/w) ratios of 100/0, 90/10, 80/20, 70/30, and 50/50 and coded as PU-2, IS1A, IS1B, IS1C, and IS1D, respectively. The isocyanate index of all the PU compositions was kept constant at 100.

IPN Characterization and Testing. Density. The density of IPNs was measured by using the water displacement method, at 27 °C. A specific gravity bottle was first filled with water and the weight of water was recorded. A weighed quantity of the solid IPN was taken into the dry specific gravity bottle and was filled partially with water. Complete wetting of the solid was ensured by applying a vacuum. The bottle was then filled completely with water, and the total weight of the water and polymer was measured. The amount of water displaced by the polymer was then calculated to obtain the volume of the IPN sample. The density was calculated from the known weight and the measured volume of the IPN. The density was accurate upto ±0.001.

Soluble Content. The IPN samples were cut into small pieces (1–2 mm) using a razor blade, and a weighed quantity was packed in Whatmann filter paper No. 1. These packets were reweighed and placed in a Soxhlet apparatus. The samples were extracted with toluene for 6 h in order to remove the soluble fractions from the IPNs. The packets were dried at 100 °C for 24 h in a vacuum oven, cooled in a desiccator, and weighed again to find the soluble content and "gel" content. The toluene extract was heated at 80 °C under vacuum for at least 4 h to remove all the toluene. The residue was then characterized by infrared spectroscopy (IR) to determine the nature of the solubilized species.

Swelling Behavior. The IPNs were cut into rectangular pieces of dimensions 2 cm × 3 cm × 0.2–0.3 cm, weighed accurately to an accuracy of 0.1 mg, and loosely wound in wire mesh. These samples were then immersed in a solvent bath for 36 h to attain equilibrium swelling. The samples were then removed from the solvent bath, wiped with tissue paper to remove the excess solvent, and weighed immediately. The swollen samples were dried in a vacuum oven at 100 °C for 24 h, cooled in a desiccator, and weighed again. The equilibrium swelling of the polymer by the solvent (v/v) was calculated as

$$\% \text{ swelling} = \left[\frac{\rho_p(W_1 - W_2)}{\rho_s W_2}\right] \times 100 \quad (1)$$

where W_1 and W_2 are the weights of the swollen and dried polymers, respectively, and ρ_s and ρ_p are the densities of the solvent and polymer, respectively. The swelling behavior of the IPNs was investigated using solvents such as ethyl acetate, toluene, and binary mixtures of ethyl acetate and toluene.

Wide Angle X-ray Diffraction (WAXD). The solid state morphology of the IPNs was studied using wide angle X-ray diffraction. Wide angle X-ray diffraction studies were carried out using the Philips PW 1730 X-ray generator unit. X-rays of 1.5418-Å wavelength were generated using a Cu Kα source. The angle of diffraction (2θ) was varied from 4 to 35°.

^{13}C NMR Spectroscopy. The structure of the IPNs and the mobility of the various chain segments were studied by solid state ^{13}C NMR spectroscopy. Due to the nonsolubility of the IPN in any solvent, ^{13}C NMR spectroscopy was carried out on the solid samples. The IPNs were cut into pieces of about 1 mm × 1 mm with a razor blade. The samples were packed tightly in Teflon sealed zirconia rotors using silica filler. All the solid state ^{13}C NMR spectra were recorded on a Bruker MSL-300 FT NMR spectrometer operating at 75.47 MHz for carbon. The samples were spun at 2–4 kHz depending on the sample packing during the experiments.

Results and Discussion

Structure Elucidation. The synthesis and chemical structure of PUP-2 have been discussed in an earlier communication.[6] The idealized structure of PUP-2 based on the stoichiometry of the reactants is shown here for reference

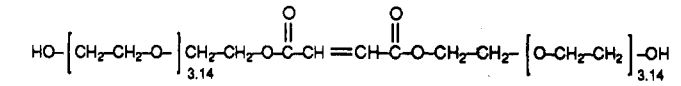

The double bond of PUP-2 is more reactive than that of natural oils such as castor oil, soybean oil, etc. due to the electron withdrawing effect of the ester group. Therefore the resin PUP-2 behaves like a semidrying oil. It forms a tough and flexible skin when cured at 60 °C. Thus, the double bonds present in PUP-2 can undergo oxidative cross-linking. The PUP-2 resin also reacts with styrene, in the presence of methyl ethyl ketone peroxide (MEKP) initiator and cobalt naphthenate accelerator at room temperature, producing a solid, elastic, infusible product. This shows that the double bonds of PUP-2 are prone to free radical attack and PS bridges can be formed between adjacent PUP-2 molecules in the PU/PS IPNs. The PUP-2–styrene copolymer was soluble in ethyl acetate. This showed that the cross-linking is not present in the product, indicating that the polyester PUP-2 did not contain more than one reactive double bond per molecule.

Similar networking or bridge formation through vinyl polymerization has been shown to occur in the unsaturated PU containing more than one grafting site per linear PU chain.[7] The formation of the cross-linked gel shows that the tendency of bridge formation between the two polymer chains is high. Thus, when the number of unsaturated sites of the PU increases, there is a greater possibility of bridge formation of a vinyl polymer between the adjacent PU network chains. These bridges act as cross-links, forming an infinite network.

In the present work, the PU network containing sites of unsaturation was formed in the presence of the styrene monomer, and then the styrene monomer was polymerized in the presence of the PU network. During polymerization of the styrene monomer with the sites of unsaturation present in the PU network, various types of situations arise. When the PS forms a covalent linkage between the two separate network chains of PU, it is termed an intranetwork bridge. If the PS chain hooks only to one network chain then it is termed a graft, and the PS chain which does not form any covalent linkage with the PU network would be present as a homopolymer of PS. Thus, the PS in the IPN would be present in one of the three forms, namely, an intranetwork bridge, a graft, or a homopolymer of PS.

The IPN formation process is a two-step reaction. It involves the PU network formation in the presence of styrene at room temperature for 24 h followed by a postcure at a higher temperature to polymerize the styrene monomer. The room temperature curing is termed α-stage curing. During the α-stage curing, styrene acts as a solvent and is entrapped in the PU network, as shown in Figure 1. After α-stage curing, all the IPNs were transparent. This implies molecular level dispersion of the styrene monomer within the PU network formed after α-stage curing. Also, all the α-stage IPNs could be handled as solid sheets, showing that the PU formation is almost complete after α-stage curing. This was confirmed by an IR study. The IR spectrum showed a strong absorption at 2250 cm^{-1} due to –N=C=O stretching vibrations. As the PU formation takes place, the isocyanate groups are consumed and the consumption of these groups can be estimated from the decrease in the absorption of the 2250-cm^{-1} band. The reaction during α-stage curing was monitored by observing the intensity of this band at specified time intervals. The results showed that 75–80% of PU formation was complete after α-stage curing (Figure 2).

Table 3. Toluene Extraction Studies of IPNs

code	PU/PS[a] (w/w)	soluble fraction (%)	gel fraction (%)
PU-2	100/00	8.00	92.00
IS1A	90/10	6.93	93.06
IS1B	80/20	9.42	90.58
IS1C	70/30	9.98	90.02
IS1D	50/50	15.37	84.63

[a] Formulation of PU–PUP-2 (4 equiv), TMP (1 equiv), and TDI (5 equiv). Formulation of PS–styrene (98%) and BPO (2%).

The PU network after α-stage curing forms a flexible network structure termed "snake cages". The transport of the styrene monomer through these cages, which determines the accessibility of the styrene radicals to the sites of unsaturation on the network, depends on the extent of PU network formation and the rigidity of the PU network. The completion of the reaction between sites of unsaturation and styrene is determined by the nature of the snake cages. During β-stage curing (see Figure 1), the free radical reaction of styrene starts. During the grafting process, the glass transition temperature of the PU network continuously increases due to an increase in the PU molecular weight and styrene reaction with the sites of unsaturation. The time at which the glass transition temperature of the polymer exceeds the curing temperature is termed the time of vitrification. At this stage, the mobility of the PU chains decreases suddenly, leading to severely hindered transport of the styrene monomer. This results in decreased accessibility of the styrene radicals to the sites of unsaturation. Thus, after this stage the remaining styrene polymerization takes place only inside the cages formed by the PU network. The higher extent of PS formation before the vitrification would increase the PS bridge formation. Thus the IPN formation process would influence the relative fractions of the three types of PS chains, namely, graft, intranetwork bridge, and homopolymer of PS.

The IPN samples coded IS1A, IS1B, and IS1C were clear, tough, and transparent elastomers, whereas IS1D was hazy. This haziness of IS1D may arise from the formation of a bigger domain size of PS (size more than the wavelength of light). The bigger domain sizes indicate formation of longer intranetwork bridges and grafts or the formation of a separate phase of the PS homopolymer.

The extraction of the β-stage cured samples was therefore carried out in toluene to estimate the amount of PS homopolymer present in the IPN, since toluene is a good solvent for PS but not for PU. The results of the extraction studies, given in Table 3, showed that the PU network (PU-2) contains 9% soluble fraction. The presence of such a high amount of soluble species is indicative of incomplete network formation. It was noted earlier that the isocyanate index of 100 was kept constant while the IPNs were formulated. However, the isocyanate index of 100 does not give complete infinite network formation, since some of the isocyanate groups react with moisture, lowering the effective isocyanate index. A complete network formation takes place around an isocyanate index of 107.[8] The incorporation of 10% PS (IS1A) reduces the soluble fraction, and on a further increase of PS content to 30% the soluble fraction remains constant around 9–10%. However, at a PS content of 50% the soluble fraction increases suddenly to 15.37%. The IR spectra of the extracts of IPNs PU-2 and IS1D were therefore studied to confirm the nature of the toluene soluble fractions.

The IR spectrum of the toluene extract of PU-2 (Figure 3) showed a strong band in the range 1000–1200 cm^{-1} and at 1264 cm^{-1} assigned to symmetrical and antisymmetrical stretching vibrations of ether (C–O–C) linkages, indicating

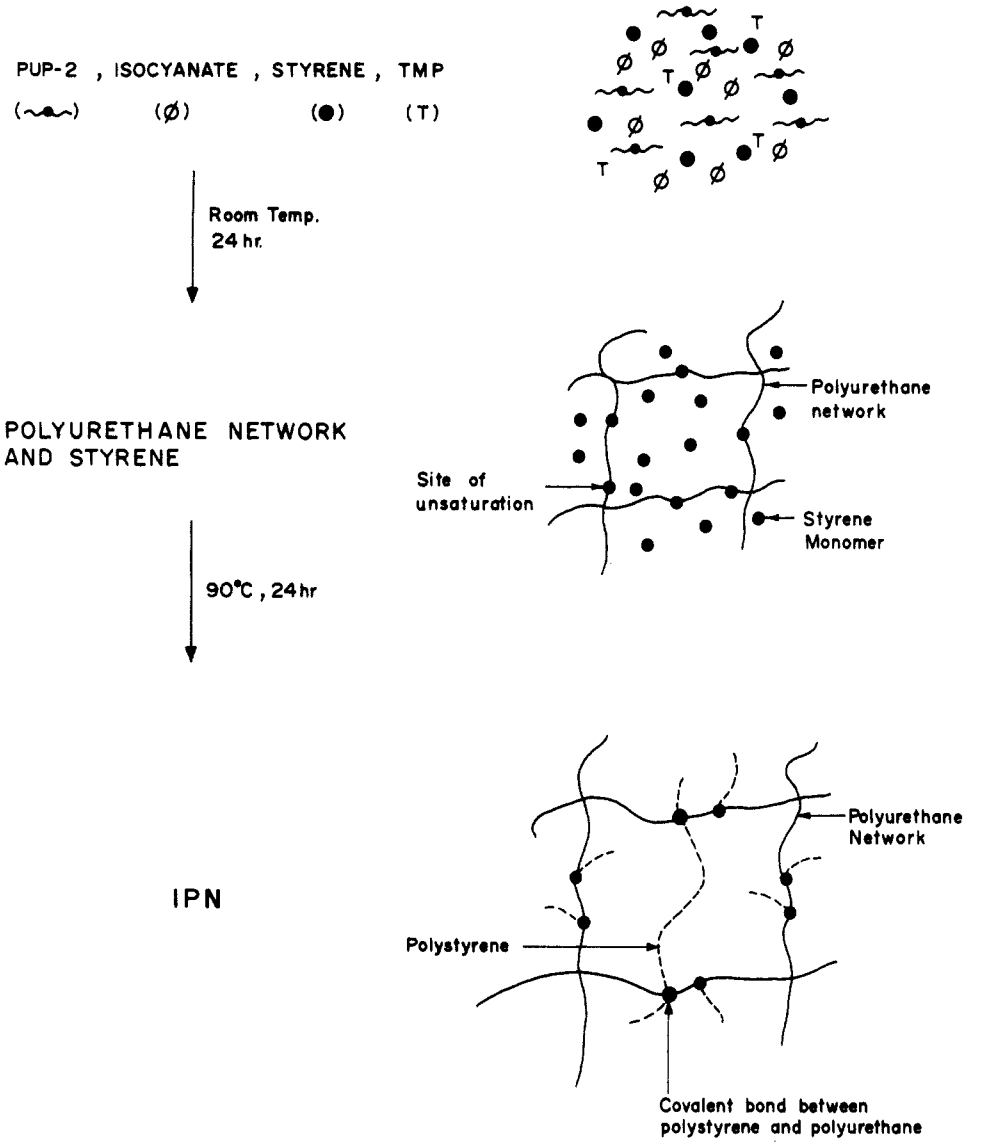

Figure 1. Interconnected IPN formation.

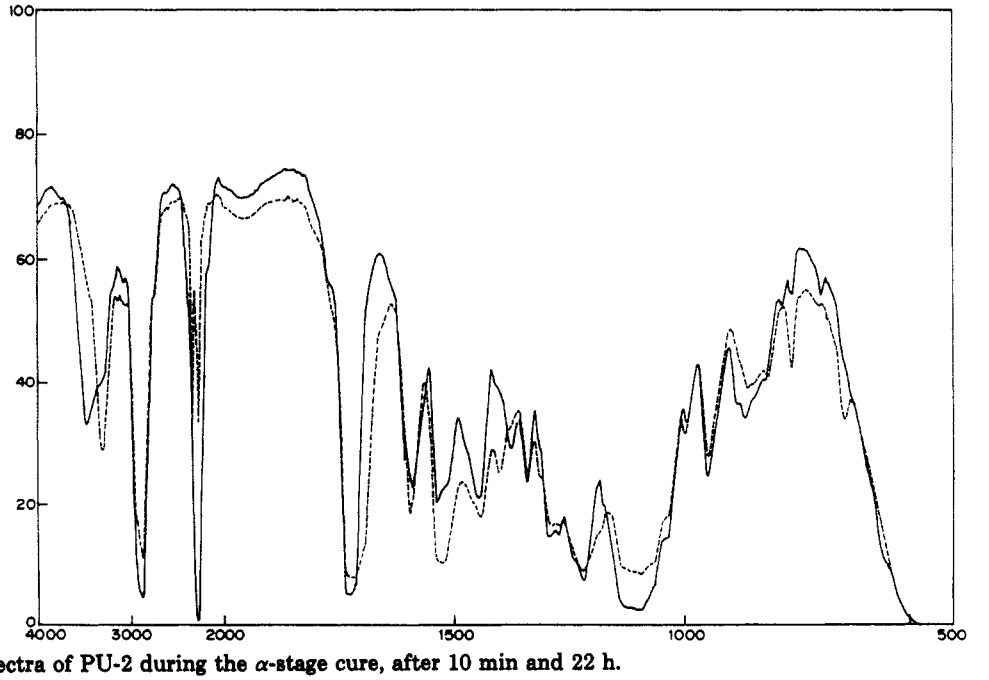

Figure 2. IR spectra of PU-2 during the α-stage cure, after 10 min and 22 h.

the presence of polyether in the extract of the PU network. A strong absorption at 1731 cm^{-1} was observed due to the stretching vibrations of the ester carbonyl group. A strong peak at 3400 cm^{-1} confirmed the presence of free hydroxyl

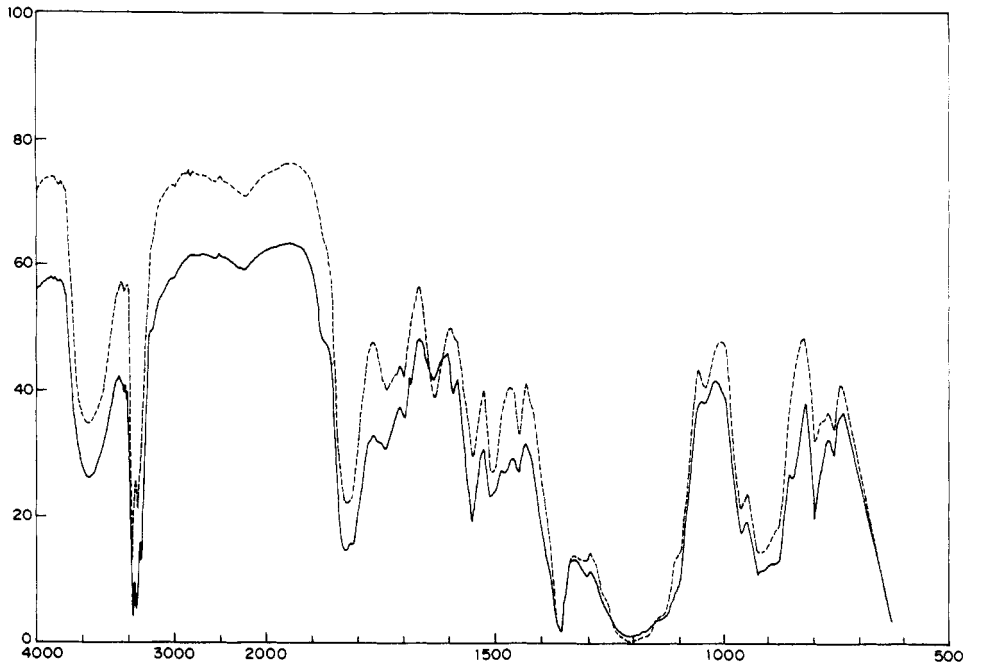

Figure 3. IR spectra of toluene extracts of PU-2 and IS1D.

groups (–OH). The band at 1600 cm^{-1} showed the presence of the aromatic ring. Thus, the IR spectrum of the toluene extract of PU-2 clearly showed that the extract was composed of the unreacted polyester PUP-2 and some amount of PU oligomers.

The IR spectrum of the toluene extract of IS1D was similar to that of PU-2 (see Figure 3). The stronger bands at 1539, 1600, and 1641 cm^{-1} indicated the presence of a slightly higher aromatic content in the IS1D extract as compared to the IPN PU-2. This showed that the IS1D extract may contain very little PS. However, the strong bands observed due to polyether and -ester indicate that the major fraction in the extract of IS1D consisted of the polyester PUP-2 or oligomeric PU chains not incorporated in the infinite network of PU. These results can be explained as follows.

The initial 10% addition of styrene showed a decrease in the soluble fraction, due to incorporation of some oligomeric PU chains of PU-2 in the infinite network through the reaction of styrene with the sites of unsaturation. The greater extent of formation of oligomeric PU in the case of the IPN IS1D is attributed to the fact that, during α-stage cure, styrene acts as a solvent and, as the concentration of styrene increases, the probability of collisions between the isocyanate and hydroxyl groups would decrease.[8] Thus, an increase in the soluble fraction was not due to the formation of a homopolymer of PS. Also, it was evident from the extraction studies that almost all the styrene reacts with the PU chains and forms PS grafts or intranetwork bridges in the PU network.

The two solvents chosen for the swelling study were such that ethyl acetate has good affinity toward both the component polymers forming the IPN (PU and PS), whereas toluene has affinity to only PS and not PU.[9] The results of swelling of IPNs in ethyl acetate, toluene, and a binary mixture of ethyl acetate and toluene at various compositions are listed in Table 4.

The IPN network forms a cage structure composed of heterogeneous chains of PU and PS. This heterogeneity was evident from the swelling of these IPNs in dimethylformamide (DMF). The opacity of all the IPNs increased on swelling (except PU-2) in dimethylformamide, and the phenomenon could be related to the presence of nonswollen

Table 4. Swelling Behavior of IPNs in a Binary Solvent Mixture of Ethyl Acetate and Toluene

	percentage of ethyl acetate in binary solvent mixture					
code	100	80	60	40	20	0
PU-2	32.86	12.59	14.17	8.38	4.80	9.04
IS1A	23.67	19.47	14.37	9.52	5.24	8.32
IS1B	41.06	32.80	25.92	23.20	14.10	10.78
IS1C	52.34	45.83	39.41	24.57	16.87	11.52
IS1D	92.46	72.92	79.24	88.50	71.13	34.94

heterogeneous chains of PS which act as light scattering centers.[10]

Since both the heterogeneous chain segments (that is PU and PS) are swollen in the presence of ethyl acetate, the equilibrium swelling of the IPNs in ethyl acetate is representative of the cage size of the IPNs. It was observed that the initial addition of 10% PS reduces the equilibrium swelling of the IPNs, while further addition of the PS results in increased equilibrium swelling.

The network structure is governed by the type and extent of cross-linking. A cross-link factor (CLF) was defined to represent the cage structure in a quantitative manner. The CLF is a number representing the cross-link density of the IPN if all the styrene was used in forming intranetwork bridges. The relationship of the CLF with various properties will indicate whether the PS is present as intranetwork bridges or as grafts.

The following assumptions were made in defining the CLF: (i) The reaction between isocyanate (–NCO) and hydroxyl (–OH) groups is complete.

(ii) Only urethane linkages (–NH–C(O)–O) are formed during the PU network formation. The additional cross-linking through the formation of allophanate, biuret, or isocyanurate linkages does not take place if the stoichiometric excess of diisocyanate groups is not present.

(iii) All the double bonds in PU are freely accessible to the styrene radicals after α-stage curing, and the reaction between the styrene and double bonds is complete.

(iv) No reaction between sites of unsaturation on adjacent PU chains takes place during the α-stage curing.

(v) The styrene monomer completely reacts with the sites of unsaturation present on the PU network and forms intranetwork bridges.

Table 5. Cross-Link Factor (CLF) and Bridge Length of IPNs

code	CLF	bridge length (SU)
PU-2	2.07	
IS1A	8.33	1.49
IS1B	7.40	3.35
IS1C	6.48	5.63
IS1D	4.63	13.40

Using these assumptions, CLF was defined as follows:

$$\mathrm{CLF} = \left[C_u\left(\frac{\mathrm{II}}{100}\right)^f + C_s + 0.5D_b\left(\frac{\mathrm{II}}{100}\right)^2 + 2E_i\right] \times 10^4 \quad (2)$$

where C_u gives the moles of PU cross-linker per gram of formulation (for example TMP), II is the isocyanate index, f is the functionality of the PU cross-linker ($f = 3$ for TMP), C_s gives the moles of styrene cross-linker per gram of formulation, D_b is the moles of double bond present in PU per gram of formulation, and E_i gives the moles of excess isocyanate groups present per gram of formulation (applicable at II > 100). At isocyanate indices of less than 100, some of the cages are not completely formed due to formation of the noninfinite network. The factors $(\mathrm{II}/100)^f$ and $(\mathrm{II}/100)^2$ signify the probability that the cross-linker of functionality f and the sites of unsaturation will act as an effective cross-link, in the case of the formation of a noninfinite network. Thus, these probabilities are valid only for the IPNs containing the PU networks formed with an isocyanate index of less than 100. If the isocyanate index of the PU network exceeds 100, then this factor should be eliminated from the equation. The amount of double bonds was normalized by multiplying with 0.5, as only 50% of the double bonds are available for reaction with styrene.[6] From a phenomenological viewpoint, the network cage size decreases with increasing CLF value.

Using the same assumptions, the average number of styrene monomer units constituting the PS bridge was calculated in terms of the moles of styrene present per mole of site of unsaturation in the PU network chains. This bridge length is expressed in terms of the number of styrene units (SU). In an actual network, one styrene unit of an intranetwork bridge length represents the stretching of adjacent PU chains by 2.4 Å. The cross-link factors (CLF) and the intranetwork bridge lengths of PS for all the IPNs are tabulated in Table 5.

The percentage swelling of the IPNs in ethyl acetate decreased linearly with increasing CLF (Figure 4). This showed that the equilibrium cage size of an IPN swollen in ethyl acetate was dependent on the sample cross-link density. Thus the IPNs contain most of the PS in the form of intranetwork bridges, rather than as grafts onto PU chains. The plain PU network (PU-2), however, showed considerably lower equilibrium swelling. Due to postcuring of PU at temperatures of 90 and 120 °C, some of the double bonds present in the PU could undergo oxidative cross-linking, thereby significantly hindering the segmental mobility and decreasing the cage size. The lower swelling of the PU network may also be attributed to the presence of hard segments of double bonds in the PU network chains and the decrease in the interaction between the solvent and the double bond containing chain segments.

The percentage swelling of the IPNs in toluene remains almost constant up to a PS content of 30%, but a large increase in swelling was observed for IS1D. This indicates a greater level of constraint of the PU network on the mobility of PS intranetwork bridges. The significant increase in the equilibrium swelling for IS1D in toluene at a PU to PS ratio of 50/50 implies that the nature of the PS bridge in IS1D is different from that in the other IPNs.

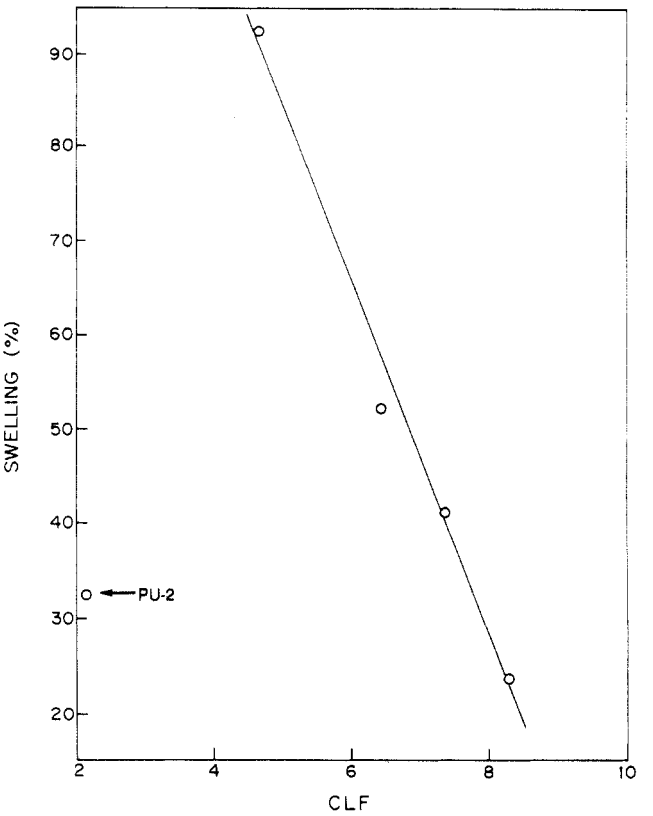

Figure 4. Dependence of equilibrium swelling of interconnected IPNs in ethyl acetate on the cross-link factor (CLF).

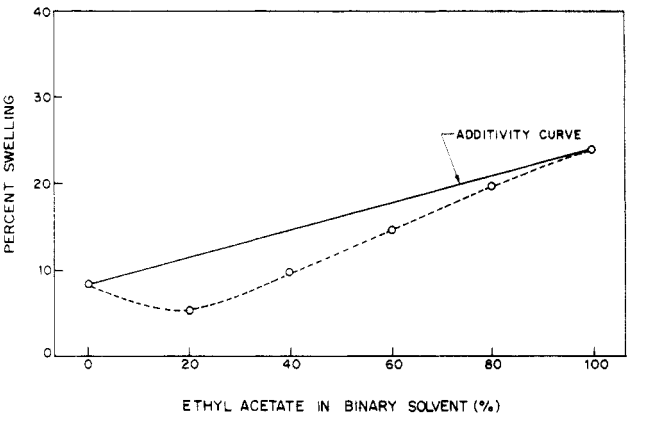

Figure 5. Swelling behavior of IS1A in a binary mixture of ethyl acetate and toluene.

In order to understand this phenomenon, the swelling studies were carried out in binary mixtures of ethyl acetate and toluene. Referring to Table 4, the equilibrium swelling increases with increasing ethyl acetate content of the mixed solvent for all the IPNs. As indicated in Figures 5–7, the variation of equilibrium swelling of the IPNs with ethyl acetate content follows the rule of additivity fairly closely for IS1A, IS1B, and IS1C. This shows that the limitation on the swelling of these IPNs in toluene was not due to the constraints on the PS chains imposed by the PU network. If it were so, a large positive deviation from the additivity curve would have been observed. This suggests that the PS chains are present in a stretched configuration and that they could not be further extended by swelling in toluene. Thus, the cage structure of IS1A, IS1B, and IS1C appears to contain the stretched PS chains as intranetwork bridges.

In the case of IS1D, a large positive deviation from the additivity curve was observed (Figure 8). This indicates that the PS chains can be swollen to a much greater extent

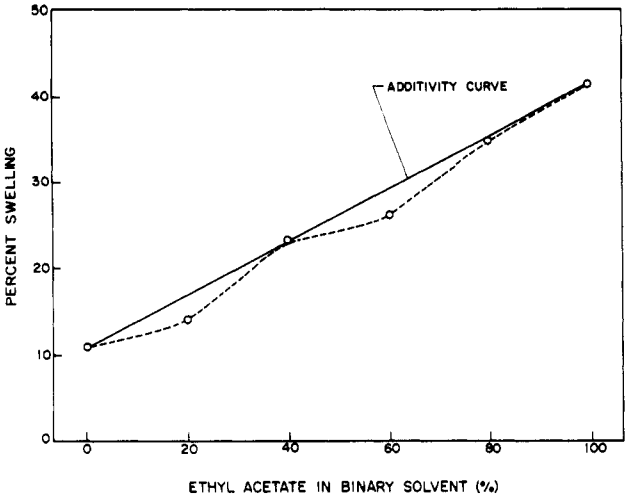

Figure 6. Swelling behavior of IS1B in a binary mixture of ethyl acetate and toluene.

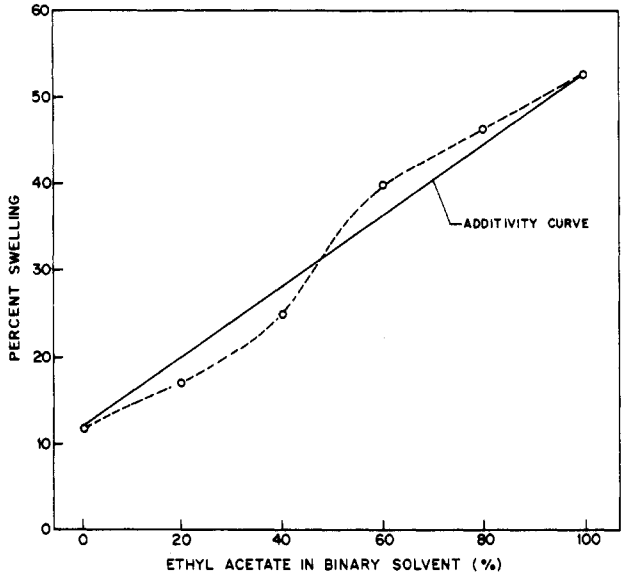

Figure 7. Swelling behavior of IS1C in a binary mixture of ethyl acetate and toluene.

if the PU constraint on them is relaxed by 20% addition of ethyl acetate in the solvent mixture. Thus the PS chains present in IS1D are not in a stretched form and they are accommodated in the PU network in the coiled configuration, which is able to swell as soon as the PU constraint is relaxed.

The wide angle X-ray diffraction study (WAXD) was carried out to investigate the solid state structure of the IPNs. The results of WAXD are summarized in Table 6. It was observed that the effective distance between the chains (d_{eff}) increases with the increasing amount of PS. A maximum in d_{eff} was observed for the IPN IS1C, having an intranetwork bridge length of 5.7 SU (Figure 9). On a further increase of bridge length to 13.4 SU, the IPN IS1D, the d_{eff} decreased significantly to a value lower than the d_{eff} of the IPN PU-2. This shows that the PS bridges which are present as stretched chains lead to stretching of the flexible PU cages, increasing the d_{eff}. In the case of IS1D, which has a bridge length of 13.4 SU, a collapsed cage morphology results. These results are consistent with the swelling behavior of the IPNs which indicated that the configuration of the PS chains in IS1D was different as compared to that in IS1A, IS1B, and IS1C.

The disorder of the polymer as indicated by half-width increased with increasing styrene content (see Table 6).

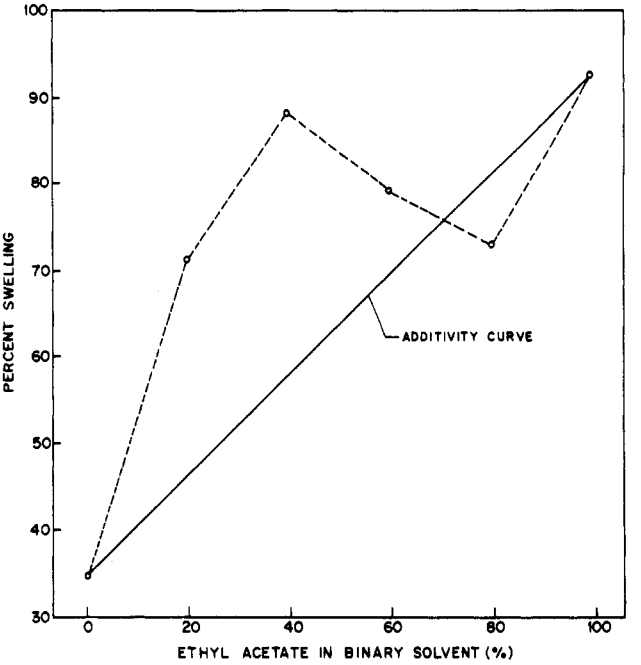

Figure 8. Swelling behavior of IS1D in a binary mixture of ethyl acetate and toluene.

Table 6. Density and Wide Angle X-ray Diffraction of IPNs

code	d_{eff} (Å)	half-width of amorphous peak (Å)	peak height (relative units)	crystallinity (relative units)	density (g/cm³)
PU-2	4.04	10.1	3250		1.2791
IS1A	4.15	10.0	2950		1.1521
IS1B	4.15	11.1	2450	6	1.1869
IS1C	4.19	11.4	2350	20	1.2097
IS1D	3.96	12.1	2000	2	1.1449
IS1D[a]	4.15	9.0	2700	14	1.1356

[a] Characteristics of IPN IS1D after given strain history.

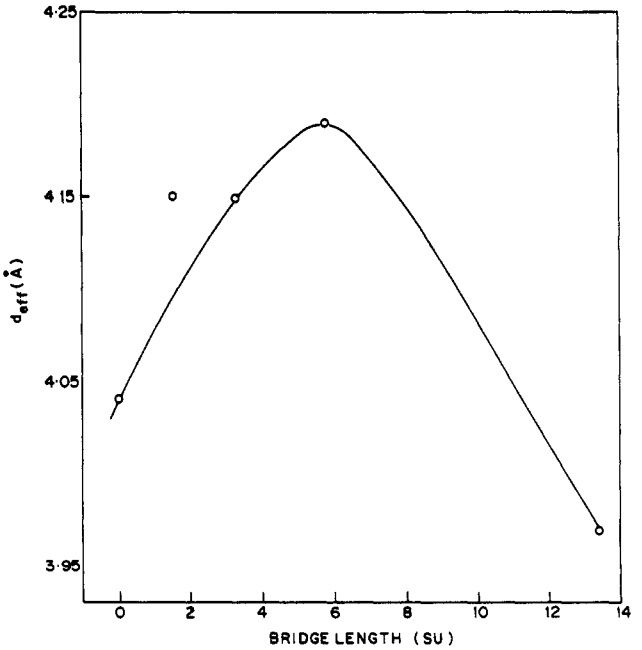

Figure 9. Dependence of effective distance between the chains (d_{eff}) on bridge length.

This indicated the formation of a broader distribution of the cage sizes with increasing intranetwork bridge length of PS.

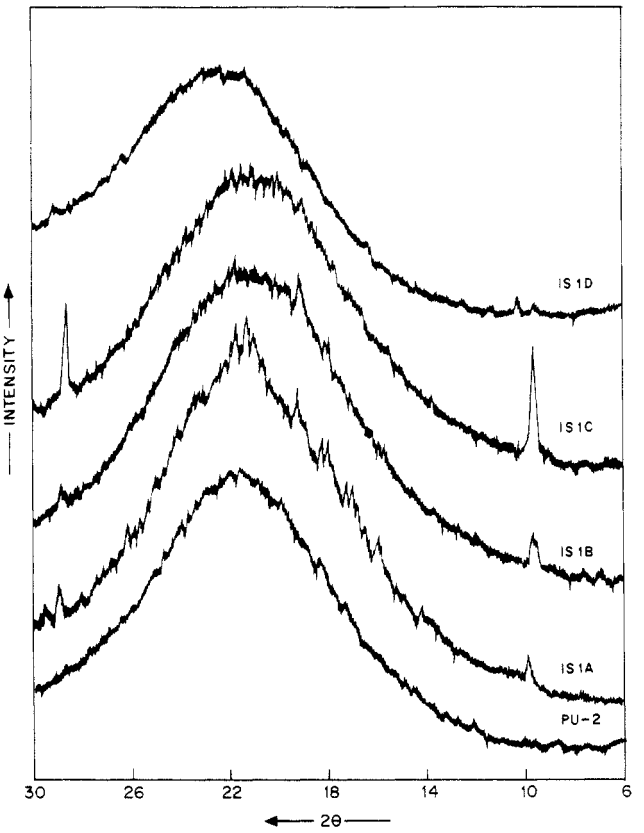

Figure 10. WAXD patterns of interconnected IPNs.

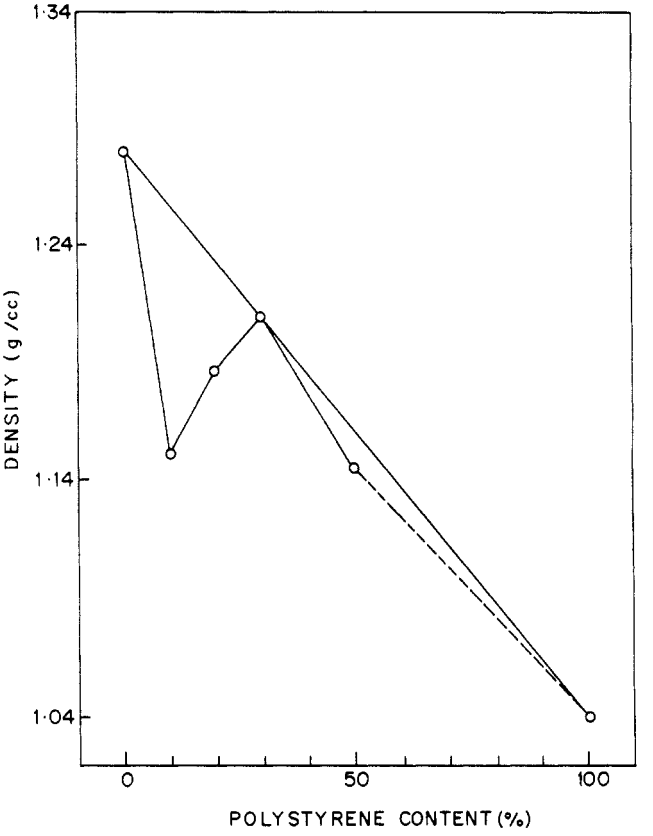

Figure 11. Density versus polystyrene content.

The conclusion concerning the stretched chain configuration of PS bridges in IS1B and IS1C is also confirmed by the observation of crystalline peaks at 9 and 29° in the WAXD scan (Figure 10). These peaks are attributed to stress induced crystallization of polyether chain segments of the PU chains, strained as a result of stretched PS bridges. Similar effects have been reported in the case of some AB cross-linked polymers such as unsaturated polyesters containing poly(ether glycols).[11] These results indicate that a PS bridge length of more than 4 SU causes sufficient stretching of PU chains to allow the PEG to form crystalline domains. This, of course, is not valid in the case of IS1D, since the PS bridges are in the coiled configuration and do not stretch the PU chains.

The densities of IPNs show a very peculiar trend (Table 6). The density of the IPN sharply decreases on addition of 10% styrene to the PU network. However, the density of the IPNs IS1B and IS1C, containing 20 and 30% styrene, increased as the styrene content was increased. A further increase to 50% styrene content resulted in a decrease of the density. When these results are compared to the additivity curve, it is evident that the density decreased sharply at a styrene content of 10% (Figure 11). Thus the IPN IS1A, containing 10% PS shows an increased free volume due to formation of PS intranetwork bridges. This has been confirmed by the WAXD results, which showed that the d_{eff} increases due to formation of the intranetwork bridges. On a further increase of the styrene content the density of the IPN increases up to a styrene content of 30% and becomes comparable to that expected by the additivity curve. Although a further decrease in density would be expected for the IPNs IS1B and IS1C, since they contain longer PS intranetwork bridges, and WAXD results have shown higher d_{eff}, there is an increased density for IS1B and IS1D. This behavior was attributed to the presence of crystalline domains of polyether chain segments developed during the IPN formation. The density of IS1D was found to be fairly close to the additivity curve, since there were no crystalline domains and it formed a collapsed cage structure.

There are two possibilities which can explain the formation of a collapsed cage structure in the case of IS1D: (i) The PU network cages are not so large that they can accommodate the PS bridges longer than 6 SU. This would force the PS chains to coil in order to accommodate themselves within the PU network. (ii) The styrene monomer content in IS1D is 50%. This may lead to formation of larger microglobules, after the α-stage curing.[12] The larger size of these microglobules may not allow the PS chains to stretch due to entanglements within the PS bridges.

In order to find out the reason for the collapsed cage morphology, relaxation studies were carried out on an Instron tensile tester. PU-2 and IS1D samples were stretched to 50% elongation, held at this elongation for 1 h, and then allowed to relax for 7 days. The WAXD scan of PU-2 does not show any change in d_{eff} and half-width of the peak after this strain history. However, in the case of IS1D, d_{eff} increased from 3.96 to 4.15 Å, accompanied by a sharp decrease in the half-width, an increase in peak intensity, and the appearance of crystalline peaks at 9 and 28° (see Table 6 and Figure 12). This result shows that an irreversible change in the cage structure of IS1D has taken place by changing the coiled configuration of the PS bridges to a stretched configuration. Thus, the following conclusions can be drawn: (i) The PU network cages can accommodate stretched PS chains present in IS1D. Thus, the coiled configuration was not due to formation of longer PS bridges. (ii) PS chains are not present as grafts, since they can stretch the PU cages. (iii) It appears that the stretching of PU cages by PS intranetwork bridges is not hindered by the formation of internal entanglements of the PS intranetwork bridges. (iv) This experiment also confirms that the stretching of PU cages by PS induces crystallization of polyether segments.

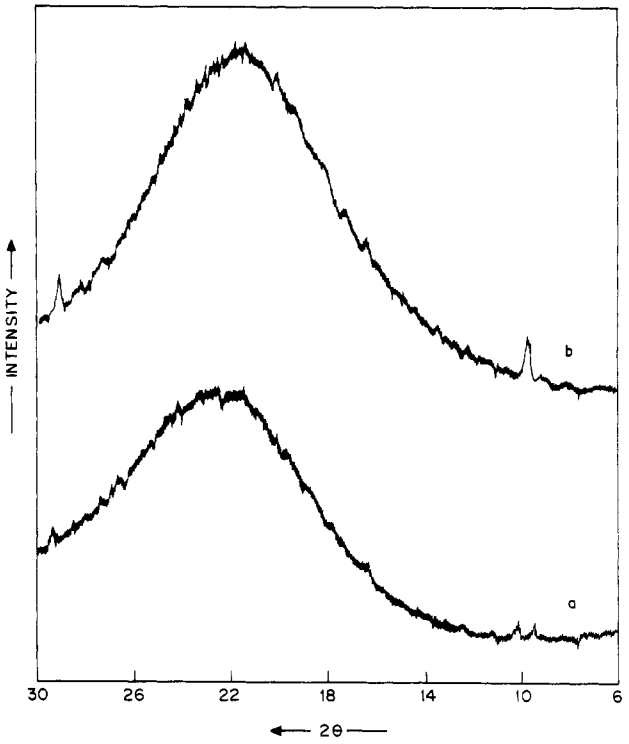

Figure 12. WAXD patterns of IS1D before and after stress relaxation.

It was evident from the swelling behavior and the solid state morphology of the IPNs (studied using WAXD) that the IPNs studied have three types of cage structures. The plain PU network, PU-2, has an amorphous cage structure. The IPNs IS1A, IS1B, and IS1C form stretched cages, and the IPN IS1D has a collapsed cage structure. The molecular motions of the chain segments forming these cages would provide important information about their structures. ^{13}C NMR spectroscopy is a tool used to study the molecular motions of the polymers. Since all the IPN samples were highly cross-linked, they could not be dissolved in any solvent. Hence, solid state ^{13}C NMR spectra of the selected IPNs reprsenting these cage structures, namely, PU-2, IS1C, and IS1D, were studied using cross polarization with the magic angle sample spinning (CP-MASS) technique. In this technique, the sample is rotated at the magic angle to obtain isotropic chemical shifts of the carbons present in the solid sample and cross polarization is used to enhance the sensitivity of the spectrum without isotope enrichment. In order to suppress the sidebands observed in the CP-MASS spectrum, it was recorded using the "total sideband separation" (TOSS) technique.

The ^{13}C NMR spectrum of PU-2 may be analyzed with respect to the probable chemical structure of the repeat unit of PU-2 (shown in Figure 13) derived from the stoichiometry of the reactants used for its preparation. The NMR spectrum of PUP-2 is shown in Figure 14, and the assignments of all the peaks are listed in Table 7. The NMR spectrum showed a peak at 17 ppm due to the methyl carbon present on the aromatic ring. A peak due to ether carbons was observed at 70 ppm (refer to the ^{13}C NMR spectrum of PUP-2 shown in Figure 14). The aromatic carbons were observed at 110 and 136 ppm. The urethane carbonyl peak was observed at 154 ppm. A peak due to unsaturated carbons, appearing at 129 ppm in the case of polyol PUP-2 (Figure 14), could not be observed separately, as it was hidden in the aromatic peak. The ester carbonyl present in PU-2 shows two peaks around 170 ppm. Two signals were observed in this region at 165 and 172 ppm.

Table 7. Assignments of ^{13}C NMR Peaks

signal (PPM)	assignment
17	$-CH_3$ carbon of TDI
41	$-CH_2$ and $-CH$ carbons of PS
70	$-CH_2$ carbons present on the polyether segment
100, 136	aromatic carbons present on TDI
127	aromatic carbons present on PS
129	$=CH-$ carbons adjacent to ester linkage
145	quaternary aromatic carbon present on PS
154	carbonyl carbon present in the urethane linkage
165	α,β unsaturated carbonyl of PUP-2
172	saturated carbonyl group of PUP-2

This shows that the carbonyl groups present in PU-2 may be in two different environments. The peaks at 165 and 172 ppm are assigned to the carbonyl on the α,β unsaturated ester and the carbonyl present on the saturated esters formed due to oxidative cross-linking of the polyester PUP-2, respectively. The peak at 43 ppm was observed due to the saturated CH groups formed as a result of oxidative cross-linking of the PUP-2 during the synthesis of PU-2. This clearly indicates that oxidative cross-linking has taken place. Thus, the lower cage size of the PU-2 observed during the sorption study can be partially attributed to the increased cross-linking in PU-2 as a result of oxidative cross-linking.

The chemical structures of IS1C and IS1D IPNs based on PU and PS networks are similar except for the relative concentrations of the various groups. The probable chemical structures of the repeat unit of the IPNs are shown in Figure 15.

The ^{13}C NMR spectrum of IS1C is shown in Figure 16. The spectrum shows all the peaks that were observed in the ^{13}C NMR spectrum of PU-2, except that the intensities of the ester carbonyl observed were different. The peak at 172 ppm was much larger than the peak at 165 ppm, indicating that the concentration of the carbonyl attached to the α,β unsaturated ester has decreased. This implies that the reaction between sites of unsaturation has taken place. Additional peaks were observed due to the presence of PS in the IPN. A peak was observed at 41 ppm due to the methylene and methine carbons present in PS. The aromatic methine carbons of PS were observed at 127 ppm along with the aromatic carbons present in PU-2. The quaternary carbon present on the PS aromatic ring was observed at 145 ppm. The ^{13}C NMR of IS1D was similar to that of IS1C (Figure 16). The intensities of the peaks observed for PU were much lower due to the lower concentration of the PU in this IPN. As a result, the signals of quaternary carbons forming carbonyl groups were lost.

The molecular motions of various carbons were studied using the dynamics of the cross polarization. The growth and decay of the ^{13}C magnetization were monitored under matched Hartmann–Hahn conditions with magic angle spinning. Using this method, proton spin–lattice relaxation times in the rotating frame ($T_{1\rho}$), which are sensitive to the proton–proton spin diffusion in the polymer, were measured. The signal intensity at different contact time data for various selected peaks was fitted with a nonlinear least squares fitting program in the following equation:[13]

$$I(\tau) = \frac{I_0}{1-\lambda}[1 - e^{-(1-\lambda)\tau/T_{IS}}]e^{-\tau/T_{1\rho}} \qquad (3)$$

where τ is the contact time, $I(\tau)$ is the signal intensity at contact time τ, and I_0 is the maximum intensity; λ was calculated as $\lambda = T_{IS}/T_{1\rho}$, T_{IS} is a measure of the cross polarization time.

The results of $T_{1\rho}$, the maximum intensity I_0, and cross polarization time T_{IS} obtained for various peaks of selected

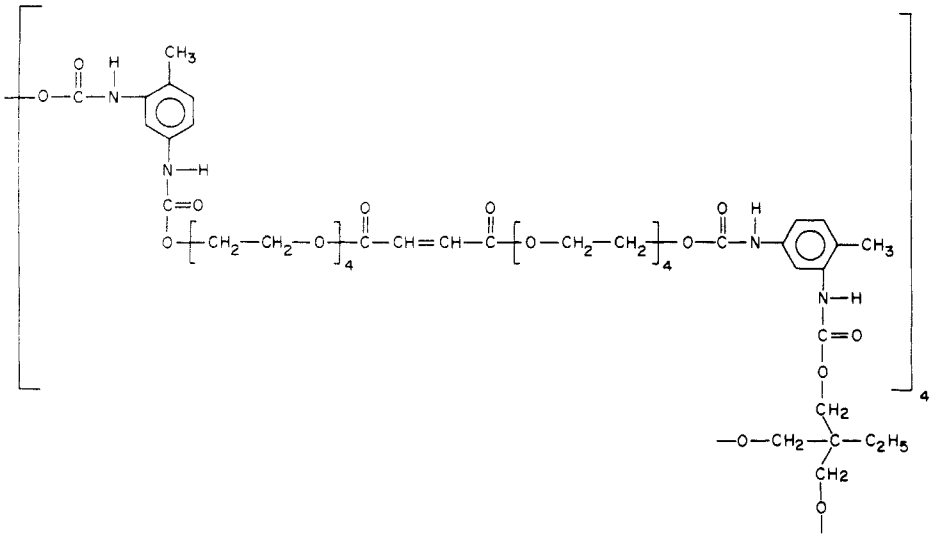

Figure 13. Probable chemical structure of a typical repeat unit of PU-2.

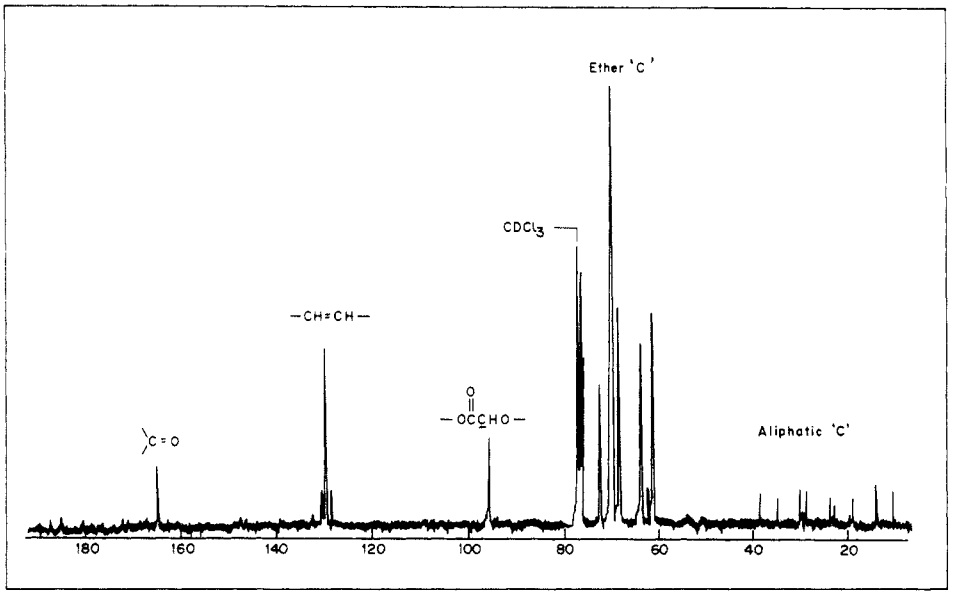

Figure 14. ^{13}C NMR spectrum of PUP-2.

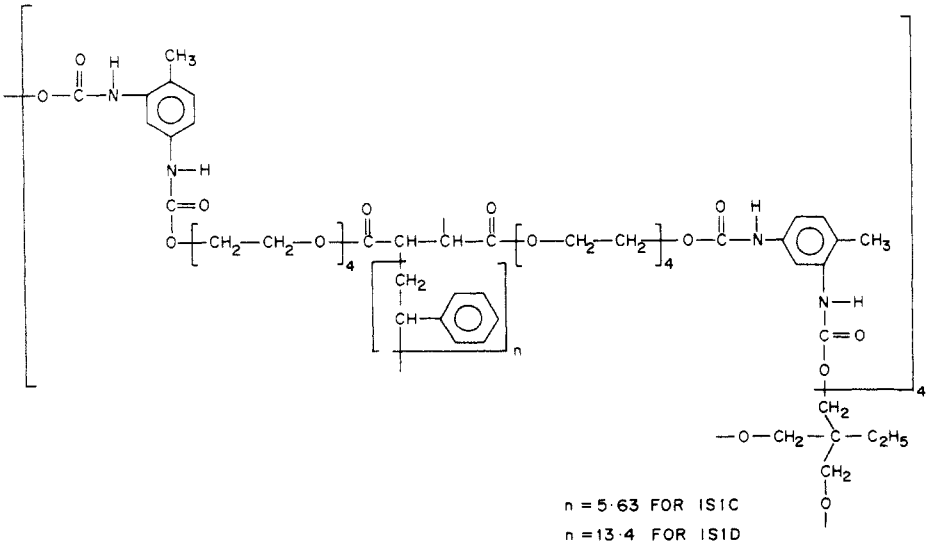

Figure 15. Probable chemical structure of a typical repeat unit of IPNs IS1D and IS1E.

samples from the least squares fitting program are summarized in Table 8. The values of $T_{1\rho}$ obtained for the PU signals in all the samples studied were in the range of 1–2 ms, whereas those for the PS signals were in the range of 5–12 ms. Thus, the proton spin diffusion does not pass across PU and PS. This, along with the earlier observation that the carbonyl group is attached to saturated carbons in the IPNs, reinforces the earlier conclusion

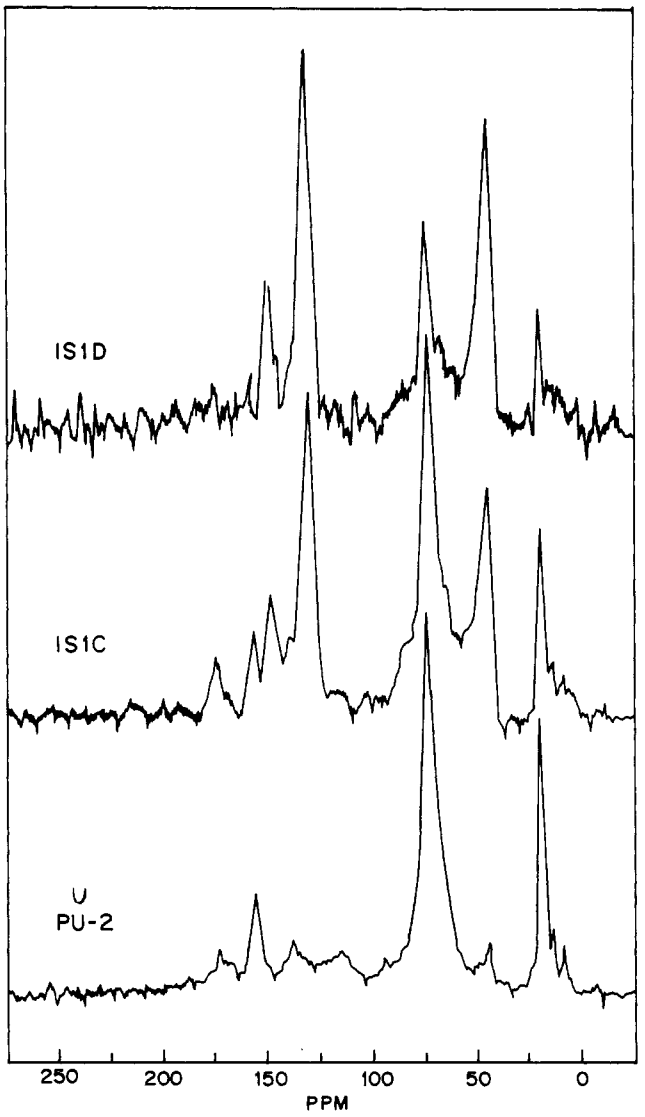

Figure 16. CP-MASS ^{13}C NMR spectrum of IPNs using the total sideband separation (TOSS) technique.

Table 8. Contact Time Analysis from Solid State ^{13}C NMR Spectroscopy

code	contact time params	signal 17 ppm	41 ppm	70 ppm	127 ppm	145 ppm	154 ppm
PU-2	I_o	66		33.8			4.7
	$T_{1\rho}$ (ms)	1.560		1.076			1.230
	T_{CH} (ms)	0.180		0.059			0.475
IS1C	I_o	5.2	12.8	27.5	9.5	2.2	3.15
	$T_{1\rho}$ (ms)	2.950	8.981	2.478	12.000	10.284	3.596
	T_{CH} (ms)	0.191	0.046	0.055	0.053	0.388	0.313
IS1D	I_o	5.87	19.67	26.5	15.6	4.3	
	$T_{1\rho}$ (ms)	2.160	7.625	1.321	7.612	4.835	
	T_{CH} (ms)	0.170	0.049	0.078	0.055	0.231	

that the IPNs contain heterogeneous cages formed by the chain segments of PU and PS. This also suggests that microdomains of PS may be present.

The $T_{1\rho}$ values of all the PU signals observed in the case of PU-2 were in the range of 1–2 ms. The values of $T_{1\rho}$ are quite short, indicating an efficient relaxation mechanism in the rotating frame due to molecular motions. Out of the three PU network signals, the one at 70 ppm is the most representative, since it emanates from the main chain. At 30% styrene content the IPN IS1C showed an increase in the $T_{1\rho}$ of the polyether chain segment from 1.3 to 2.1 ms. Thus, in the case of IS1C there was an increased constraint on the mobility of the polyether chain

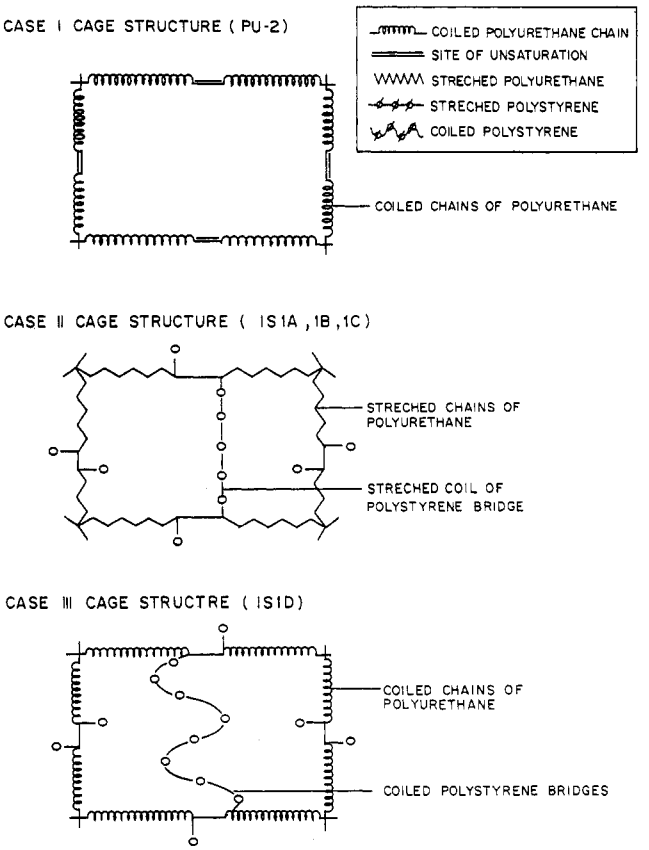

Figure 17. Proposed model for the cage structures of interconnected IPNs.

segments. This may be attributed to the formation of strained PU network cages as a result of the stretched configuration of the PS bridges in IS1C, as concluded from the swelling and WAXD data. A subsequent decrease in the $T_{1\rho}$ of the polyether segment in IS1D is indicative of greater mobility of the polyether chain segments. It may be recalled that the PS chains in IS1D are hypothesized to be in the coiled configuration from the swelling behavior and WAXD studies. The coiled form of the PS bridges would not strain the polyether chain segments, thereby making them more mobile as compared to the IPN IS1C.

The $T_{1\rho}$ values of the PS signals observed in both the IPNs IS1C and IS1D were longer than those observed for the PS homopolymer, indicating restricted motion of the PS chain segments in the IPNs formed. This shows that the PS intranetwork bridges in the IPNs are constrained. The $T_{1\rho}$ measurements show that the relaxation of PS bridges present in the IPN IS1D is faster than those present in the IPN IS1C. Thus the PS bridges present in IS1D are less constrained as compared to the PS bridges present in IS1C. This is consistent with the earlier findings, which show that the PS bridges in the IPN IS1C are in the stretched configuration while those in the case of IS1D are in the coiled configuration. A similar observation was made in the case of castor oil–polyurethane (COPU) and PS based IPNs by Ku and co-workers.[14] The proton spin–lattice relaxation time in the rotating frame ($T_{1\rho}$) is more sensitive to the mobilities in the mid-kilohertz range while the spin–spin relaxation times (T_1) are sensitive in the high frequency range. The initial experiments investigating the T_1's of the IPNs have shown that the T_1 of the PS methylene carbon decreases from 28 to 14 s as the configuration of PS bridges in the IPNs was changed from stretched to collapsed coils.

Proposed Model for the IPN Structure

On the basis of the results of the swelling studies, wide angle X-ray diffraction, and the solid state ^{13}C NMR spectroscopy, it is proposed that the following three types of network cage structures would represent the interconnected IPNs: (i) The PU network structure, PU-2, is composed of cages formed from amorphous coiled PU chain segments (Figure 17). These coiled cages may be partially linked by oxidative cross-linking of the double bonds. (ii) A heterogeneous cage structure of the IPNs IS1A, IS1B, and IS1C is formed by linking two flexible PU chain segments through intranetwork PS bridges, present in a stretched configuration (Figure 17). These stretched PS bridges lead to straining of the flexible PU chain segments during formation of the cage structure. The strain induced ordering would lead to crystallization of adjacent polyether chain segments, as observed in IS1B and IS1C. The strain induced crystalline morphology becomes predominant as the bridge length of PS increases. (iii) In the case of IS1D, the PS chains are coiled and a collapsed cage structure is formed (Figure 17). The IS1D showed irreversible deformation after the tensile relaxation experiment, and it was evident from WAXD results that the collapsed cages were transformed into stretched cages showing crystalline morphology.

Acknowledgment. We wish to thank Sudhir Kulkarni for useful discussions and help rendered during the course of the investigations. The help rendered by S. Ganapathi and P. R. Rajmohan during ^{13}C NMR investigations is gratefully acknowledged. S.B.P. thanks the Council of Scientific and Industrial Research, India, for financial support.

References and Notes

(1) (a) Thomas, D. A.; Sperling, L. H. In *Polymer Blends*; Paul, D. R., Newman, S., Eds.; Academic: New York, 1978; Vol. 2, Chapter 11. (b) Manson, J. A.; Sperling L. H. *Polymer Blends and Composites*; Plenum: New York, 1976; Chapter 8. (c) Sperling, L. H. *Interpenetrating Polymer Networks and Related Materials*; Plenum: New York, 1981.

(2) (a) Scarito, P. R.; Sperling, L. H. *Polym. Eng. Sci.* **1979**, *19*, 297. (b) Touhsaent, R. E.; Thomas, D. A.; Sperling, L. H. *J. Polym. Sci.* **1974**, *46C*, 175. (c) Touhsaent, R. E.; Thomas, D. A.; Sperling, L. H. In *Toughness and Brittleness of Plastics*; Deanin, R. D., Crugnola, A. M., Eds.; Advances in Chemistry Series No. 154; American Chemical Society: Washington, DC, 1976.

(3) Frisch, H. L.; Frisch, K. C., Klempner, D. *Polym. Eng. Sci.* **1974**, *14*, 646.

(4) (a) Devia, N.; Manson, J. A.; Sperling, L. H.; Conde, A.; *Macromolecules* **1979**, *12*, 360. (b) Devia, N.; Manson, J. A.; Sperling, L. H.; Conde, A. *Polym. Eng. Sci.* **1979**, *19*, 869, 878. (c) Devia, N.; Manson, J. A.; Sperling, L. H.; Conde, A. *J. Appl. Polym. Sci.* **1979**, *24*, 569.

(5) Kumar, V. G.; Rao, M. Rama; Guruprasad, T. R.; Rao, K. V. C. *J. Appl. Polym. Sci.* **1987**, *34*, 1803.

(6) (a) Pandit, S. B. Ph.D. Thesis, submitted to University of Poona, 1992. (b) Pandit, S. B.; Nadkarni, V. M. *Ind. Eng. Chem. Res.*, in press.

(7) (a) Beachell, H. C.; Paterson-Buck, J. C. *J. Polym. Sci.* **1969**, *A7*, 1873. (b) Beachell, H. C.; Blumstein, R.; Paterson, J. C. *J. Polym. Sci.* **1969**, *C22*, 569.

(8) Tabka, M. T.; Weidmaier, J. M.; Mayer, G. C. *Macromolecules* **1989**, *22* (4), 1826.

(9) Brandrup, J.; Immergut, E. H. *Polymer Handbook*, John Wiley and Sons Inc.: New York, 1975.

(10) Tager, A. *Physical Chemistry of Polymers*; Mir Publishers: Moscow, 1978.

(11) Boenig, H. V. *Unsaturated Polyesters: Structure and Properties*: Elsevier Publishing Co.: Amsterdam, 1964.

(12) (a) Adachi, H.; Kotaka, T. *Polym. J.* **1982**, *14* (5), 3791. (b) Adachi, H.; Nishi, S.; Kotaka, T. *Polym. J.* **1983**, *15*, 985.

(13) Mehring, M. *Principles of High Resolution NMR in Solids*; Springer Verlag: New York, 1983.

(14) Wen-Hsiung Ku; Jeng-Li Liang; Kuo-Tung Wei; Hsin-Tzu Liu; Chung-shing Huang; Suh-Yun Fang; Wen-guey Wu. *Macromolecules* **1991**, *24*, 4605.